Optical and Quantum Electronics **35:** 75–84, 2003.

An experimental work on optical component based on D-fiber/slab evanescent coupling structure

M. SALIH DINLEYICI
İzmir Institute of Technology, Electrical and Electronics Engineering Department, Urla-İzmir 35437, Turkey (E-mail: sdinleyi@likya.iyte.edu.tr)

Received 15 December 2001; accepted 16 August 2002

Abstract. Fiber/slab coupler structure has been exploited as a passive in-line optical fiber component for functions of filtering, intensity modulating and switching by many researchers. In this work a device based on the elliptic core D-fiber and polymer slab waveguide is proposed and its fabrication is experimentally investigated. The device is constructed by placing the polymer slab on the top of the flat side of the D-fiber, and then they are tested for transmission characteristics and polarization preserving properties for various configurations. The geometrical uniformity of the device is examined under Scanning Electron Microscope for the purpose of device performance evaluation. Potential usage of this device as an all-optical switch is also discussed at the end.

Key words: D-fiber/slab coupler, D-fiber evanescent coupler, all-optical components

1. Introduction

In fiber-based optical networks ultrahigh bandwidth links require technologies to support optical signal operations such as filtering, modulating and switching; furthermore, forwarding and routing the optical packages at terabit wire rates. Some of these functions might be implemented by means of evanescent coupled fiber/slab geometry that has been studied by many researchers (Marcuse 1989; Marcuse *et al.* 1992; Andreer *et al.* 1994; McCallion *et al.* 1994; Raizada and Pal 1996; Dinleyici and Patterson 1997, 1998; Jai 2001). In these works standard telecommunications optical fibers (circular core and cladding) and crystals (LiNbO, ZnSe etc.) or polymers have been studied. Intensity modulator, bandpass filters, optical logics and switching devices are proposed. Another application of this type device is bragg grating assisted coupler which uses Bragg grating between two optical waveguides to control coupling coefficient (Dinleyici 2000). Generally all these devices might be combined with photorefractive materials to make control of the device possible by means of another light (De Souze *et al.* 1999). Or using electro-optic material it is possible to design tunable devices that are controlled by applied external electrical field (Raizada and Pal 1996).

In the fabrication of these kinds of devices the fiber core is exposed to a planar waveguide by removing the fiber cladding at the desired thickness. A fiber half block, which is typically made from a quartz slab, holds the fiber in a curved groove and then this block is polished. Next a slab waveguide is formed on the top of this exposed region of the fiber by means of either depositing a polymer or attaching a crystal slab waveguide. This device exhibits a periodic bandpass or bandstop characteristics depending upon the slab waveguide parameters. Inherently this kind of devices exhibit low polarization sensitivity due to asymmetry introduced by the slab waveguide and the circular nature of the optical fiber geometry (nonpolarization holding optical fiber). In this work the first time an elliptic core D-fiber and a polymer slab waveguide is used to construct an evanescent coupler. Then, various transmission characteristics and polarization properties are investigated. The potential of this device as an all-optical switch is also emphasized.

2. Determining resonance frequency

Interaction of modes from alike waveguides has been interest of many researchers for a long time. In the fiber/slab geometry the dominant mode of the optical fiber can be coupled with one of the slab modes, which are in continuum nature due to boundless in one of the transverse direction (Dinleyici and Patterson 1998). Determination of the resonance wavelength of evanescent coupler made of a circular core optical fiber and an slab waveguide has been studied by many researchers exploiting either coupled mode theory (CMT) analysis (Marcuse *et al.* 1992; Andreev *et al.* 1994) or full/partial (quasi) vectorial approaches (McCallion *et al.* 1994; Dinleyici and Patterson 1997, 1998; Jai *et al.* 2001). The CMT approach makes use of the isolated modes of the waveguides to determine the resonance point with a certain tolerance. However, a rigorous vectorial approach exists with a penalty of computation complexity to provide full vectorial solution (McCallion *et al.* 1994; Jai *et al.* 2001). In our knowledge there is no any work dedicated to the elliptic core D-fiber evanescent coupler. The resonance points obtained in this experimental work will be compared with predictions obtained from eigenvalue equation of the slab solved for weakly guiding approximation of elliptic core fiber.

Under the weakly guiding approximation and low ellipticity even and odd modes of the elliptic core fiber are degenerate and solutions are provided in Dyott (1995). The propagation constant (effective index) of the fundamental mode is used in the slab waveguide self-consistency equation and solved for the resonance wavelengths following the procedure of Andreev *et al.* (1994) and Dinleyici and Patterson (1998). Here, the superstrate (outside of the slab) will be taken air ($n = 1.0$) and index liquid ($n = 1.46$) as in the experiment.

The resonance points for various superstrate are compared with the experimental results and discussed with the fabrication parameters in the following section.

3. D-fiber evanescent coupler fabrication

The device proposed in this work makes use of D-shape cladding of the optical fiber shown in Fig. 1. D-fiber (Ecore-930623A, polarization holding optical fiber manufactured by Andrew Co., having cladding refractive index 1.475 and $\Delta n = 0.035$, 40 dB/m extinction for polarization) core is close to the flat surface, the nearest point between the core and the flat surface is about 8 μm.

Therefore, the fiber core can be reached by etching (removing) the cladding from all directions. The experimental setup used for etching is shown in Fig. 2. Here, the light from a He–Ne laser source is launched into the fiber to excite the fundamental mode and some higher modes. Acid bath is prepared with 6:1 solution of hydrofluoric acid in water.

The detector output is recorded against time at the computer; a typical etching curve (power versus time) is shown in Fig. 3. Here, the output power is normalized to nonetched fiber maximum output power, which depends on the power launched from the laser source. The etching time is very sensitive to the temperature and number of samples in the bath. Therefore, six samples and one monitoring optical fiber are used in each etching group.

During the etching process, first of all the silica boundary layer and then the cladding of the fiber (having a refractive index of about 1.475) is replaced by the acid/water solution with an index of about 1.33. When acid reaches the evanescent field region, most of the power in the fundamental mode will be

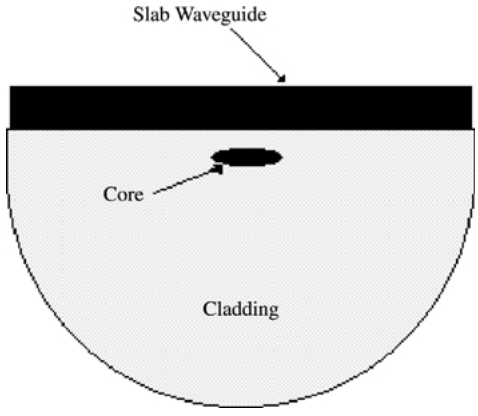

Fig. 1. Cross section of D-fiber with slab waveguide.

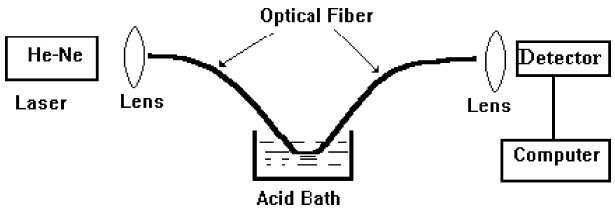

Fig. 2. The setup for etching.

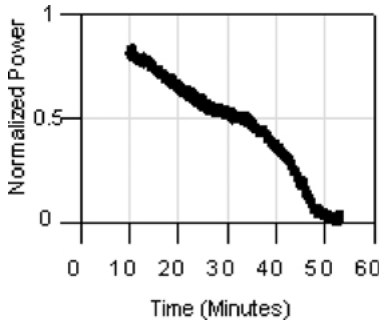

Fig. 3. A typical etching curve.

coupled into the unbounded higher order modes, which are propagating through partially acid/water solution covered optical fiber. The power in the higher order modes either excited by the He–Ne laser or coupled from the acid/water region will spread out since not confined as tight as the fundamental mode, i.e., not bounded. Indeed very little power may be coupled back into the fundamental mode after the acid bath region, however; this will not be on the level of concern. Also, a good explanation for etching D-fiber can be found in Dyott (1995).

After etching the optical fiber, it is ready to form a polymer slab waveguide on the flat side of the D-fiber. An apparatus with a microscope slide shown in Fig. 4 is used. Under a microscope the flat side of the fiber is aligned and glued on the microscope slide. Then, this slide with pigtails is placed on a cardboard disk as shown in Fig. 4. In this work we have used a polymer called benzophenone tetracarboxylic dianhydride oxydianiline with 1.52 refractive index to form the slab waveguide. One drop of the polymer is placed at the center of the slide on the etched fiber region and then the disk spun at various speeds around 2000 rpm in order to get different thickness for the slab waveguide. Next, the samples are cured in an oven at 176°C for 30 min.

The experimental setup for testing the samples is shown in Fig. 5. The tunable laser Ti:Sapphire laser is used to scan the samples 840–885 nm range. The output of titanium sapphire laser is kept constant by lowering the power

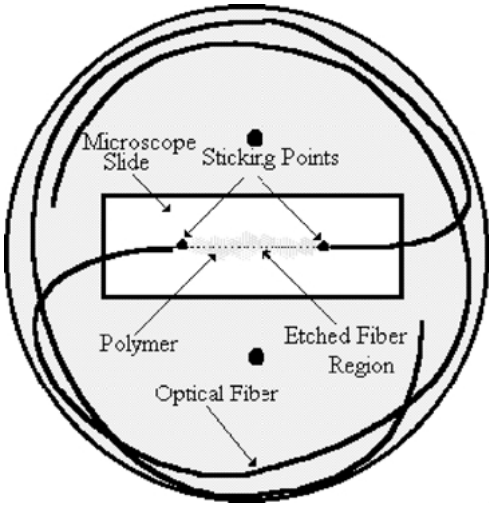

Fig. 4. Apparatus for spin coating.

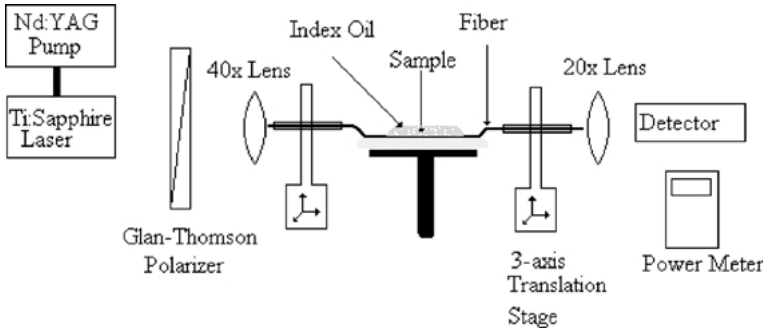

Fig. 5. Experimental setup for device testing.

into milliwatts by means of Glan–Thomson polarizer; therefore the power is in the dynamic range of the detector at the fiber output. Using the procedure outlined above many samples are prepared, however, some of the samples are damaged at the various stages of experiments due to mechanical mishandling etc. Some of these survived to be tested showed very noisy characteristics therefore, a few samples are in fact good. First of all, calibration measurements of output power versus wavelength are performed in the given spectral range 840–885 nm at the beginning and the end of the experiment, which has revealed that the laser power is not constant over the range. These power calibration curves are averaged and smoothed by curve fitting to an 8th order polynomial to remove noise components, and then this curve is used for the calibration of the data taken for the samples. Transfer characteristic is related to the geometry of the etched fiber by examining a few samples under

Scanning Electron Microscope (SEM) comparing with the power remained in the fiber after these samples are tested.

4. Results

The first and second samples are prepared by etching the fiber 67 and 60 min with spinning at 2175 and 1560 rpm respectively.

The second sample exhibits a bandpass characteristic with 11-nm bandwidth (FWHM) while the first sample's resonance point is out of the spectral range of the source towards lower wavelengths as shown in Fig. 6. The second sample is broken after the experiment for investigation of geometrical structure using SEM and it is found that the core is located about 4 μm away from the slab/cladding boundary. Also, the slab waveguide thickness is not uniform and ranging from 4 to 8 μm across the 70 μm width of the flat surface. At the vicinity of the core this thickness is about 4 μm. A draw obtained from the SEM image showing the slab geometry is given in Fig. 7.

The resonance point for this sample can be read 852 nm from the Fig. 6. The similar result can be derived from the theoretical analysis, which predicts 853 nm for 4.25 μm thick slab waveguide with an index of 1.52. In Fig. 6 the transmitted power is observed to extend into the longer wavelength region more than into the shorter wavelength region. This might also be due to wavelength dependence of power coupling into the optical fiber.

The third sample is prepared with spinning 2300 rpm. The power transmission curves are shown in Fig. 8 for two types of superstrate; normal air and index oil with refractive index of 1.46. Since the index of this liquid is very sensitive to the temperature this situation is also taken into consideration in the experiment.

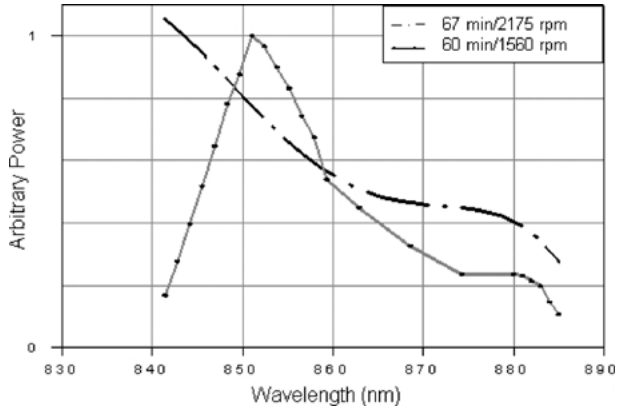

Fig. 6. Power transmission characteristic of the first sample.

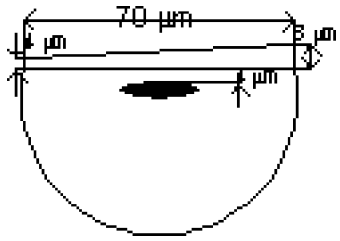

Fig. 7. Slab/fiber geometry of the second sample.

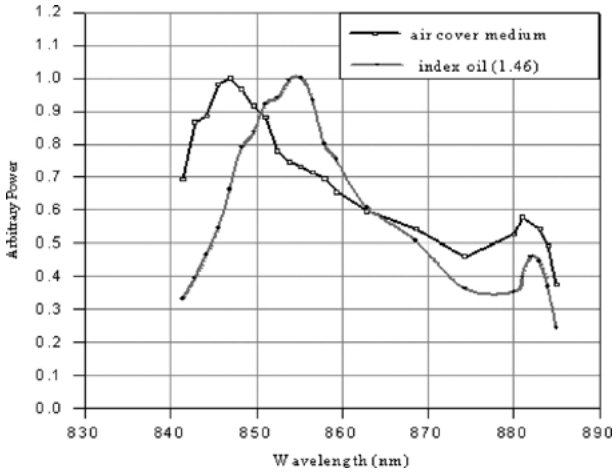

Fig. 8. Power transmission characteristics of second sample.

Each curve in Fig. 8 has two peaks, and with the second peaks at the longer wavelength side having lower transmission coefficient. The second peaks are due to TE modes since they shift very little with the index oil as observed in the other experimental reports (De Souze *et al.* 1999) too and also, have lower peak values. In the experimental setup, a Glan–Thomson polarizer has been used to reduce the input power, so that the light launched into the fiber is highly polarized. However, the orientation of the core ellipse, which defines the direction of the TE and TM modes at the input, was not aligned very precisely to this polarization; therefore, the input power is unequally split into TE and TM modes. Consequently, the peak values corresponding to the TE and TM modes are expected to have different maximum values.

Observing Fig. 9, which was obtained for the same sample after a sheet polarizer is placed at the fiber input and approximately aligned to the TE polarization direction, further supports this argument.

This alignment is accomplished by observing the polarization at the fiber output; since the fiber preserves polarization, the far field output polarization

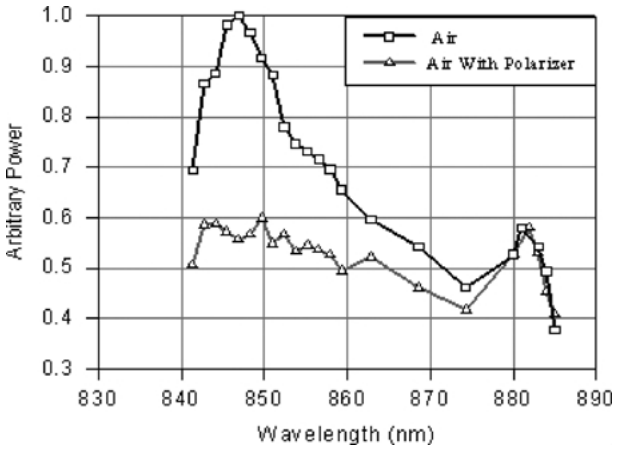

Fig. 9. Power transmission characteristic of third sample with polarizer.

state indicates the state in the fiber. It is seen in Fig. 9 that for this case the TM mode is sharply attenuated by the polarizers while the TE mode has as much power as in the case of no polarizes. These curves show approximately 30 nm bandwidth (FWHM) for TM modes, but TE modes can not be properly measured, because the peak is too close the end of spectral region of the source and noisy. The resonance wavelengths can be read from Fig. 8 that 846 nm for TM mode and 881 nm for TE mode. The numerical results predict that TM modes are resonate at 844 nm and TE modes are resonate at 882 nm for the slab thickness 3.2 μm. These results are good agreement with the experimental ones.

The resonance points shift to the longer wavelengths with changing the refractive index of the superstrate (overlay) as stated in a number of papers. Here, in this experiment TM modes shift 100 nm while TE modes show very little change by changing the superstrate index from 1.0 to 1.46. However, the numerical calculations expect 175 nm shift in the TM modes and 39 nm in TE modes.

For the first sample the resonance points of TE and TM modes are computed at 817 nm and 791 nm respectively having that the polymer slab thickness is about 4.07 μm. These points are out of the spectrum that Ti:Sapphire source provide. The thickness of these samples is computed by linearly interpolating the spinning rates and the thickness of the other samples. Therefore, the thickness of the slab waveguide can be tuned precisely by controlling the rpm of the spin coating.

The examination of the second sample under SEM has revealed that the polymer slab waveguide was not properly formed by this simple technique. One reason for this might be due to slightly mis-alignment of the flat side of D-fiber during polymer forming. Moreover, the density of the polymer might

be a factor too. The flatness of the slab waveguide in the direction of the fiber should also be considered for a better performance. The effective length of the device, which is the region where the fiber and the slab waveguide modes interact effectively, should be long enough to allow the power completely extracted for a given configuration as explained in Passaro (2000).

These results show that the D-fiber evanescent coupler might be constructed by this simple technique for various applications. However, the process should be improved in order to form a uniform slab waveguide on the flat side of the D-fiber and various other polymers should be investigated for the better performance.

5. Conclusion

Obviously this technique can be improved for the better and acceptable device performance (bandwidth and power transmission characteristics), i.e., a few nanometer bandwidth. The results also showed that the important design parameter slab thickness can be precisely controlled by means of the spin coating revolution speed (rpm) because there is an almost linear relation between these two variables.

Furthermore, high electro-optic coefficient polymers can be used for tunable devices as suggested by many researchers (Marcuse 1989; Marcuse *et al.* 1992; Andreev *et al.* 1994) or polymers showing highly nonlinear coefficients can be exploited for the purpose of light controlled devices via fourwave mixing (FWM). Applying the FWM mixing at the slab fiber junction might improve the FWM switching performance further (Johnstone *et al.* 1992). This device also fits very well as a node in an array structure for the purpose of optical cross connects. Generally this geometry is very suitable to implement arrayed structures by cascading the nodes on the slab waveguide.

Polarization holding properties of elliptic core D-fiber is preserved in this device structure and this property makes it attractive for coherent lightwave communication.

Another important application of this kind of devices may be all-optical switching which uses grating assisted coupling between the slab waveguide and D-fiber. Here, a reflective grating can be formed in the slab waveguide by interfering two highly coherent light beams, which counter propagating in the slab waveguide.

Acknowledgements

Author would like to thank Prof Dr B.K. Mandal for invaluable suggestions in the subject of polymer waveguide forming. Author is also indebted to Prof Dr David B. Patterson.

References

Andreev, A.Tz., K.P. Panajotov and E.I. Karakoleva. *IEEE Photonics Technol. Lett*. **6** 1238, 1994.
Marcuse, D., F. Ladouceur and J.D. Love. *IEE Proc. J*. **139** 117, 1992.
Marcuse, D., *J. Lightwave Technol*. **7** 122, 1989.
Dinleyici, M.S. and D.B. Patterson *J. Lightwave Technol*. **16** 2034, 1998.
Dinleyici, M.S. and D.B. Patterson *J. Lightwave Technol*. **15** 2316, 1997.
Raizada, G. and B.P. Pal. *Opt. Lett*. **21** 399, 1996.
Jaj, I.A., P. Xie and T. Mishima. *Opt. Commun*. **187** 7, 2001.
McCallion, K., W. Johnstone and G. Fawcett. *Opt. Lett*. **19** 542, 1994.
Dinleyici, M.S. *Fiber and Integrated Opt*. **19** 87, 2000.
De Souze, P.C., G. Nader, T. Catunda, M. Muramatsu and R.J. Horowicz. *Opt. Commun*. **163** 44, 1999.
Dyott, R.B. *Elliptical Fiber Waveguides*, Artech House, 83, 1995.
Passaro, V.M.N. **18** 973, 2000.
Johnstone, W., G. Thursby, D. Moodie, R. Varshrey and B. Culshaw. *Electron. Lett*. **28** 1364, 1992.